In a recent paper,[1] design tables for a wideband elliptic-function bandstop transmission-line filter have been described. The method of computation starts from a lumped-element (LE) filter specified in the catalogue of Saal. Several unit elements (UE), with unit normalized characteristic impedance, are put in cascade with this LE filter. By a succession of Kuroda's transformations, these UE are shifted within the LE 2-port, in order to yield a structure convenient for implementation with transmission lines (TL).

The UE in cascade constitute an all-pass 2-port. Hence the original LE filter and the resulting TL filter have the same attenuation characteristic. Although the latter is undoubtedly elliptic, it does not offer the optimum selectivity attainable with the same element cost, because the filtering ability of the UE in cascade is not made use of when their characteristic impedances are restricted to unity. An improved design lifts this restriction and optimizes directly the TL filter characteristic.

Consider the filter given in Fig. 3 of Schiffmann and Young.[1] Let $H(p)=f(p)/g(p)$ be the transmittance of a 2-port, where $f(p)$ and $g(p)$ are polynomials of degree n and m, respectively. For the filter of Fig. 3,[1] $n=4$ and $m=5$. Adding a cascade of four UE yields the filter of Fig. 5[1] with $n=8$ and $m=9$. With this value of m it is possible to locate nine attenuation zeros in the passband instead of the five attenuation zeros provided by the design of Schiffmann and Young.[1]

The approximation process can be made according to the theoretical approach of Ozaki and Ishii[2] or can be realized by a computer program yielding a Chebyshev behavior in both passband and stopband. The only particularity is the compulsory location of two double roots of f at ± 1. The two other pairs of roots of f are located in order to maximize the minimum of attenuation in the stopband. Simultaneously the nine attenuation zeros are selected to minimize the maximum of attenuation in the passband.

This process has been applied to the "trial" filter described in Schiffmann and Young.[1] With all other factors kept constant (0.28 dB of ripple in the band or 0.25 maximum reflection coefficient, selectivity specified by bandwidth ratios 1 and 0.34), the stopband attenuation obtained is 64.9 dB compared to 41.2 dB in Schiffmann and Young,[1] a discrimination increase of 23.7 dB. The curves are compared in Fig. 1. There is a small difference in the ripple (less than 0.02 dB) due to rounding-off errors.

It is interesting to observe that the attenuation ratio (64.9/41.2) is surprisingly close to the ratio of effective filtering components (11/7). This points to the fact that the filtering potential of the UE in cascade equals that of the UE in the stubs. Neglecting this potential amounts to a proportional lack in selectivity.

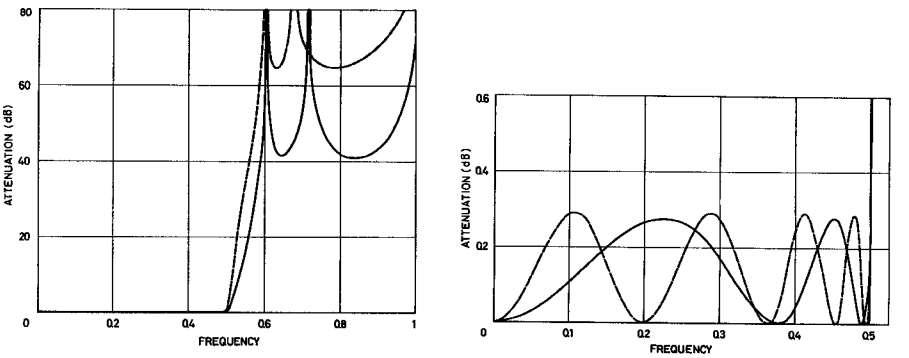

Fig. 1. (a) Attenuation of the Schiffmann and Young filter (solid line) compared to the attenuation of the optimum filter (dotted line). The frequency axis refers to the imaginary part of the dimensionless complex variable obtained through Richards' mapping. (b) Detail of the passband attenuation. The optimum filter presents one attenuation zero at the origin and four pairs of attenuation zeros versus two pairs for the Schiffmann and Young filter.

From other designs, it appears that the proportionality of the discrimination to the number of effective filtering components is a general rule. This can be justified on the basis of an image parameter theory. Although the actual designs are made on an effective behavior basis, it is well known that the image parameter theory gives a good estimate of the global performances. To take care of the UE in cascade, Soldi[3] has introduced the concept of the $\frac{1}{2}K\psi$ section. This section has an image attenuation which is formally the same as that of a m-derived, lumped parameter half section, with a value of m larger than unity, contrary to the common m-derived section. Nevertheless, this section brings a substantial amount of attenuation in the stopband. As far as the sections, with different m values, produce discriminations of the same order of magnitude, the total discrimination is proportional to the number of effective filtering sections.

The new design has been synthesized with the same structure as represented in Fig. 1 of Schiffmann and Young.[1] The values of the elements, labeled with the same notations, are

$$Z_1 = 0.6837 \qquad Z_{34} = 1.553$$
$$Z_{12} = 1.535 \qquad Z_4' = 0.9972$$
$$Z_2' = 0.6919 \qquad Z_4'' = 1.884$$
$$Z_2'' = 2.135 \qquad Z_{45} = 1.416$$
$$Z_{23} = 1.659 \qquad Z_5 = 0.7103.$$
$$Z_3 = 0.4231$$

As a bonus, the improved design method has also restricted the range of characteristic impedances to $2.135/0.4231 = 5.05$ compared to $5.147/0.445 = 11.6$ in Schiffmann and Young.[1]

To summarize, the solution obtained here presents some significant improvements with respect to that obtained in Schiffmann and Young.[1] The importance of the UE in tandem was emphasized in Ozaki and Ishii:[2] the last example given[2] meets similar attenuation requirements as the trial filter[1] with five UE instead of nine. An optimum design relies on a slightly more sophisticated method which requires a computer. As the number of UE in tandem lies between one third and one half of the total number of elements, their filtering capability should be utilized whenever a computer is available.

L. Fraiture
J. Neirynck
MBLE Research Lab.
Brussels, Belgium

Higher Order Modes in Rectangular Coaxial Waveguides

A precise determination of the characteristic impedance of rectangular coaxial waveguides has been recently undertaken by Cruzan and Garver [1] and it is well known that these structures have many applications in the design of shielded striplines, varactor mounts, etc. While their operation is, in general, confined to the TEM mode, there are instances when higher-order modes must be taken into account; the effect of the latter on striplines has been studied by Oliner [2], but there appears to be no record of a similar investigation applicable to rectangular coaxial waveguides.

In what follows, a symmetrical structure will be considered, i.e., the centers of the inner and outer conductors will be assumed to coincide. Furthermore, reference will be made to TE_{nm} and TM_{nm} modes to conform with standard notation for single-ridge waveguides [3] as well as rectangular waveguides.

Inspection of Fig. 1 shows that when the subscripts m or n or both are even, the planes of symmetry MN or KL or both are electric walls and the field pattern may be deduced from that of the corresponding single-ridge waveguide. On the other hand, the $TE_{2n+1,2m+1}$ and $TM_{2n+1,2m+1}$ ($n=0, 1, 2, \cdots$,

Manuscript received January 24, 1967; revised April 4, 1967.

[1] B. M. Schiffmann and L. Young, "Design tables for an elliptic-function bandstop filter ($N=5$)," *IEEE Trans. Microwave Theory and Techniques*, vol. MTT-14, pp. 474–482, October 1966.

[2] H. Ozaki and J. Ishii, "Synthesis of transmission-line networks and the design of UHF filter," *IRE Trans. Circuit Theory*, vol. CT-2, pp. 325–336, December 1955.

[3] M. Soldi, "Solution of the approximation problem for distributed constant filters by means of Darlington reference filters," *Alta Frequenza*, vol. 34, pp. 340–348, May 1965.

$m=0, 1, 2, \cdots$) mode patterns cannot be studied in this manner. Furthermore, while the TE_{n0} modes in ridge waveguides have been very adequately studied [3], [6], published information concerning other modes is either incomplete or not available.

The solution of the problem may be readily accomplished (without recourse to finite difference methods) using a procedure due to Butcher [4] as well as Collins and Daly [5].

Thus, in order to determine the cutoff frequencies of $TM_{2n+1,2m+1}$ modes, it is necessary to solve the wave equation for the cross section TLBNPF (Fig. 1) subject to the boundary conditions which require the longitudinal component of the electric field intensity E_z to vanish along PFT and LBN while the normal derivative $\partial E_z/\partial n$ is equal to zero along PN and TL. Furthermore, it is advantageous [5] to divide the cross section into two rectangular areas and to match the fields along the boundary FF'. Using subscripts 1 and 2 to refer to the cross sections TLBF' and PFF'N, respectively, we find that

$$E_{z1} = \sum_r^\infty \phi_{1r} \sinh p_{1r}\left(\frac{x}{a} - \frac{1}{2}\right) \cdot \sin\frac{r\pi y}{b} \qquad 0 < y < \frac{b}{2}$$
$$r = 1, 3, 5, \cdots, \text{odd} \quad (1)$$

$$E_{z2} = \sum_m^\infty \phi_{2m} \cosh p_{2m}\frac{x}{a} \sin\frac{m\pi y}{d} \qquad 0 < y < d \qquad d \neq 0$$
$$m = 1, 2, 3, \cdots \quad (2)$$

where

$$p_{2m}^2 = -k^2a^2 + \left(\frac{m\pi a}{d}\right)^2$$
$$p_{1r}^2 = -k^2a^2 + \left(\frac{r\pi a}{b}\right)^2 \qquad k = \frac{2\pi}{\lambda_c} \quad (3)$$

and λ_c represents the cutoff wavelength. Continuity of E_z along the boundary implies that $E_{z1}=E_{z2}$ when $x=s/2$, $s\neq a$; when the equation is multiplied by $\sin n\pi y/b$ and both sides integrated from 0 to $b/2$ we find that, noting the orthogonality properties of trigonometric functions,

$$\phi_{1n}\sinh p_{1n}\left(\frac{s}{2a} - \frac{1}{2}\right) = \frac{4d}{b}\sum_m^\infty \phi_{2m}K_{mn}\cosh p_{2m}\frac{s}{2a} \quad (4)$$

where

$$K_{mn} = \frac{1}{d}\int_0^d \sin\frac{m\pi y}{d}\sin\frac{n\pi y}{b}\,dy. \quad (5)$$

Similarly, continuity of H_y along the boundary FF' requires that $\partial E_{z1}/\partial x$ be equated to $\partial E_{z2}/\partial x$ at $x=s/2$; when the resulting equation is multiplied by $\sin m\pi y/d$ and both sides integrated from 0 to d, we find that

$$\sum_r^\infty \phi_{1r}p_{1r}K_{mr}\cosh p_{1r}\left(\frac{s}{2a} - \frac{1}{2}\right) = \frac{1}{2}\phi_{2m}p_{2m}\sinh p_{2m}\frac{s}{2a}. \quad (6)$$

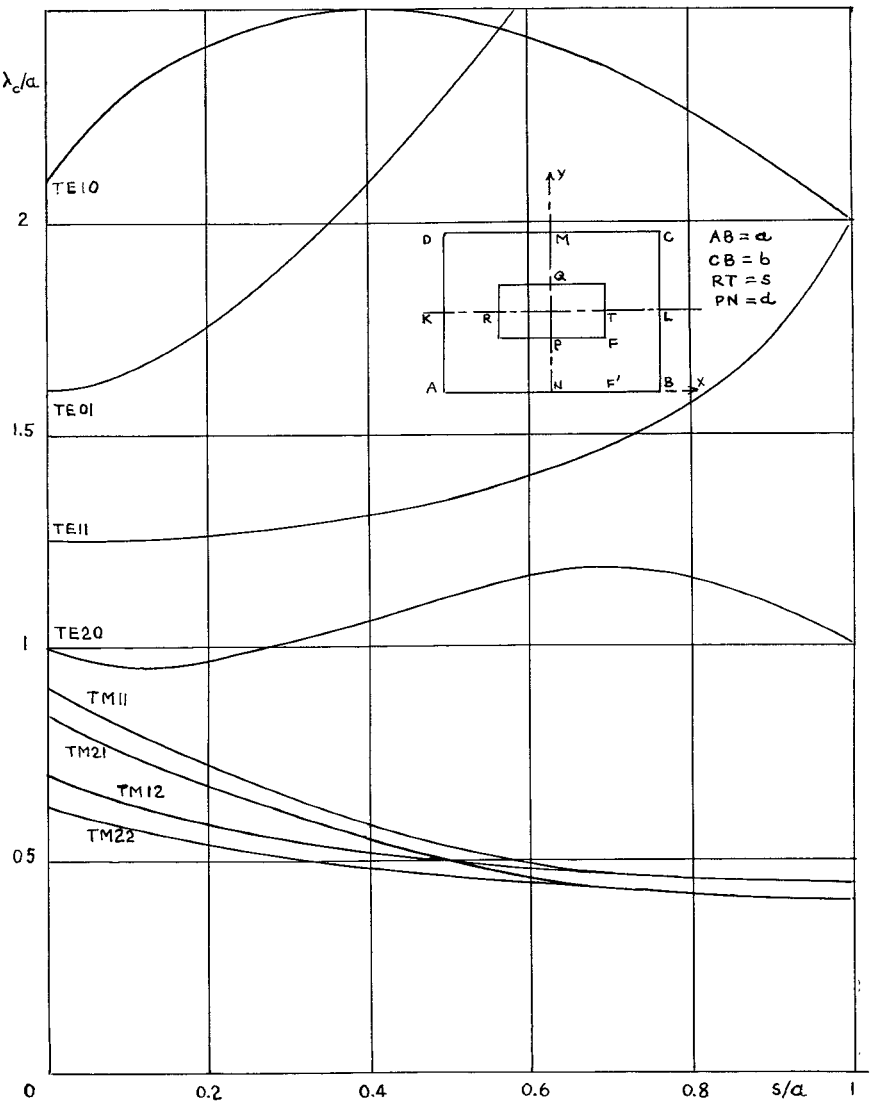

Fig. 1. Typical mode characteristics of rectangular coaxial waveguides ($b/a=0.8$, $2d/b=0.6$).

Eliminating ϕ_{2m} from (4) and (6) we have

$$\sum_{\substack{n=1,3\\ \text{odd}}}^\infty \sum_{\substack{r=1,3\\ \text{odd}}}^\infty \phi_{1r}a_{nr(oc)} \cdot \cosh p_{1r}\left(\frac{1}{2} - \frac{s}{2a}\right) = 0 \quad (7)$$

where

$$a_{nr(oc)} = \frac{8dp_{1r}}{b} \cdot \sum_{m=1}^\infty \frac{K_{mr}K_{mn}\coth p_{2m}\frac{s}{2a}}{p_{2m}} + \delta_{nr}\tanh p_{1r}\left(\frac{1}{2} - \frac{s}{2a}\right) \quad (8)$$

and $\delta_{nr}=1$ if $n=r$ whereas $\delta_{nr}=0$ otherwise. Equation (7) has a solution only if the determinant vanishes and the cutoff frequencies may be deduced by setting

$$\det[a_{nr(oc)}] = 0. \quad (9)$$

Let us designate $a_{nr(ec)}$ an expression obtained from (8) by letting the summation extend over all even n and r (commencing with $r=n=2$); similarly, let $a_{nr(ot)}$ refer to (8) subject to coth $p_{2m}(s/2a)$ being replaced by tanh $p_{2m}(s/2a)$, etc.

Then we find that the cutoff frequencies of various modes can be deduced by solving the following equations

$$TM_{2n+1,2m}: \det[a_{nr(ec)}] = 0 \quad (10)$$
$$TM_{2n,2m+1}: \det[a_{nr(ot)}] = 0 \quad (11)$$
$$TM_{2n,2m}: \det[a_{nr(et)}] = 0. \quad (12)$$

The cutoff frequencies of TE modes may be obtained in an analogous manner if the magnetic field intensity H_z in regions 1 and 2 is represented as suitable Fourier series and then the continuity of H_z and E_y is satisfied along the boundary FF'. Introducing a notation

$$b_{nr(oc)} = 8\frac{d}{bp_{1r}\Delta_r} \cdot \sum_{m=0}^\infty \frac{p_{2m}C_{rm}C_{mn}\coth p_{2m}\frac{s}{2a}}{\Delta_m} + \delta_{nr}\tanh p_{1r}\left(\frac{1}{2} - \frac{s}{2a}\right) \quad (13)$$

where

$$C_{mr} = \frac{1}{d}\int_0^d \cos\frac{r\pi y}{b}\cos\frac{m\pi y}{d}\,dy \quad (14)$$

$\Delta_m = 2$ if $m = 0$, $\Delta_r = 2$ if $r = 0$, and $\Delta_m = \Delta_r = 1$ otherwise and finally letting the subscripts o, e, c, and t have the same significance as applied to both a_{nr} and b_{nr} (but for the fact that even summation includes $r = n = 0$), we find that the cutoff frequencies of various modes may be deduced by solving the following equations

$$TE_{2n+1,2m+1}: \det[b_{nr(oc)}] = 0 \quad (15)$$

$$TE_{2n+1,2m}: \det[b_{nr(ee)}] = 0 \quad (16)$$

$$TE_{2n,2m+1}: \det[b_{nr(ot)}] = 0 \quad (17)$$

$$TE_{2n,2m}: \det[b_{nr(et)}] = 0. \quad (18)$$

Evidently (10) to (12) and (16) to (18) may be used to study modes in single-ridge waveguides; (16) and (18) are, with some changes in notation, due to Collins and Daly [5].

It can be shown that the cutoff frequencies of all modes reduce to those of the rectangular waveguide as the dimensions of the inner conductor tend to zero. Thus, for example, for $TM_{2n+1,2m}$ modes we note that when $2d/b = 1$, then for all s (including $s = 0$) we have $p_{1r} = p_{2m}$, $K_{mr} = K_{mn} = \frac{1}{2}$ subject to $n = r = m$. Hence (10) reduces to

$$\left[\coth p_{1r}\frac{s}{2a} + \tanh p_{1r}\left(\frac{1}{2} - \frac{s}{2a}\right)\right] \times \text{const.} = 0 \quad (19)$$

which has a solution

$$\coth\frac{p_{1r}}{2} = 0 \quad (20)$$

and hence

$$\lambda_c = 2/\sqrt{\left(\frac{2n+1}{a}\right)^2 + \left(\frac{2m}{b}\right)^2}$$

$$n = 0, 1, 2, \cdots, \quad m = 1, 2, \cdots. \quad (21)$$

Equations (20) and (21) hold for $TE_{2n+1,2m}$ modes as well subject to $m = 0, 1, 2, \cdots$.

Similarly, when $TM_{2n,2m+1}$ and $TE_{2n,2m+1}$ modes are considered, we find that the plane $s = 0$ represents an electric wall and hence, for all values of $2d/b$, the determinant vanishes when

$$\tanh\frac{p_{1r}}{2} = 0 \quad (22)$$

and

$$\lambda_c = 2/\sqrt{\left(\frac{2n}{a}\right)^2 + \left(\frac{2m+1}{b}\right)^2}. \quad (23)$$

With reference to the curves when $s = 0$, for the TE_{01} mode $\lambda_c/a = 1.6$ and for the TM_{21} mode $\lambda_c/a = 0.848$.

Furthermore, $TM_{2n,2m}$ and $TE_{2n,2m}$ modes have two planes of symmetry $s = 0$ and $2d/b = 1$ and hence (22) applies in conjunction with

$$\lambda_c = 2/\sqrt{\left(\frac{2n}{a}\right)^2 + \left(\frac{2m}{b}\right)^2}. \quad (24)$$

Specifically, when $s = 0$, for the TE_{20} mode $\lambda_c/a = 1$ and for the TM_{22} mode $\lambda_c/a = 0.625$.

Finally, $TE_{2n+1,2m+1}$ and $TM_{2n+1,2m+1}$ modes have no planes of symmetry. When $s = 0$ and $2d/b = 1$ determinants (10) and (15) diverge; however, in practice when $2d/b = 1$, $b/a = 0.8$ and $s = 0.03$, numerical computations reveal the presence of a root $\lambda_c/a = 1.249$ while for the rectangular waveguide corresponding to $s = 0$, $2d/b = 1$, we find that $\lambda_c/a = 1.249$ as well.

When $d = 0$ and $s = a$, the coaxial structure is transformed into two waveguides and the equations cannot be expected to hold in general.

However, a study of the field pattern suggests that when s approaches a, in the limit the ratio λ_c/a of a coaxial TE_{11} mode tends to that of a TE_{10} mode in a rectangular waveguide, viz., $\lambda_c/a = 2$; similarly, λ_c/a of the coaxial TE_{12} mode tends to that of a TE_{11} mode in a rectangular waveguide of reduced height (when $b/a = 0.8$, $2d/b = 0.6$, replacing b by $0.3b$ we find that $\lambda_c/a = 0.466$) etc. Numerical calculations confirm these conjectures.

The convergence with respect to m in both (8) and (13) is quite rapid and both expressions vary asymptotically as $0(m^{-3})$. Furthermore, the cutoff frequencies are primarily determined by a single diagonal term of $\det[a_{nr}]$ or $\det[b_{nr}]$ and a 3×3 determinant is likely to be adequate for most purposes.

It is of interest to note that the above procedure entails no approximations other than those inherent in the assumption that the walls are lossless. Normalized cutoff wavelength ratios λ_c/a obtained by Pyle [6] for the TE_{10} mode ($b/a = 0.45$) were compared with those obtained by the evaluation of 2×2 and 3×3 determinants of (16) and truncating the summation with respect to m after 8 terms. Typical results are shown below.

d/b	s/a	2×2 Determinant	3×3 Determinant	Reference [6]
0.2	0.2	3.769	3.920	3.985
0.2	0.9	2.892	2.916	2.961
0.8	0.2	2.121	2.140	2.163
0.8	0.9	2.051	2.051	2.057

Some λ_c/a characteristics of a rectangular coaxial waveguide (such that $b/a = 0.8$, $2d/b = 0.6$) are presented in Fig. 1.

An examination of these curves shows that as the frequency is increased and the propagation of higher-order modes becomes possible, the TE_{10} (TE_{01}) mode appears followed by the TE_{11} and TE_{20} modes (the TM_{11} mode precedes the TE_{20} mode for some combinations of $2d/b$ and s/a subject to the same aspect ratio $b/a = 0.8$); it also shows under what conditions two modes have the same cutoff frequency and hence velocity of propagation.

ACKNOWLEDGMENT

All computations were carried out on the Monash University CDC3200 computer.

L. GRUNER
Dept. of Elec. Engrg.
Monash University
Clayton, Victoria
Australia

REFERENCES

[1] O. R. Cruzan and R. V. Garver, "Characteristic impedance of rectangular coaxial transmission lines," *IEEE Trans. Microwave Theory and Techniques*, vol. MTT-12, pp. 488–495, September 1964.
[2] A. A. Oliner, "Theoretical developments in symmetrical strip transmission line," in *Proc. of the Symp. on Modern Advances in Microwave Techniques*, vol. 4. Brooklyn, N. Y.: Polytechnic Press of the Polytechnic Institute of Brooklyn, 1954.
[3] S. Hopfer, "The design of ridged waveguides," *IRE Trans. Microwave Theory and Techniques*, vol. MTT-3, pp. 20–29, October 1955.
[4] P. N. Butcher, "A theoretical study of propagation along tape ladder lines," *Proc. IEE* (London), pt. B, vol. 104, pp. 169–176, March 1957.
[5] J. H. Collins and P. Daly, "Orthogonal mode theory of single-ridge waveguides," *J. Electronics and Control*, vol. 17, pp. 121–129, August 1964.
[6] J. R. Pyle, "The cutoff wavelength of the TE_{10} mode in ridged rectangular waveguide of any aspect ratio," *IEEE Trans. Microwave Theory and Techniques*, vol. MTT-14, pp. 175–183, April 1966.

Numerical Solution of TEM-Line Problems Involving Inhomogeneous Media

Both empirical and analytical methods have been used in the past to evaluate the characteristic impedance of transmission lines supporting the TEM mode of wave propagation. Most of the analytical methods are rather tedious for practical use, employ approximations, or are restricted to simple configurations.

Therefore, in recent years, numerical methods for the solution of the Laplace equation in two dimensions in finite difference form using digital computers have been developed. From the Laplace equation, the potential distribution over the cross section of the transmission line is obtained, and integrating the potential gradient along a path enclosing the inner conductor yields the capacitance per unit length. This capacitance is used to determine the characteristic impedance and phase velocity of the line. Green[1] and Schneider[2] have investigated these procedures and used them to obtain interesting and useful results. For further information, these two papers or the numerous references cited in them should be consulted. The error involved in the assumption that a transmission line with inhomogeneous medium supports a pure TEM mode is a fraction of a percent up to frequencies of several gigahertz for configurations with similar dimensions to those under investigation in this correspondence.

With the use of integrated circuits on ceramic substrates suspended between two parallel ground planes, the knowledge of the characteristic impedance and phase velocity of such transmission lines in inhomogeneous media is necessary. The purpose of this correspondence is to investigate these two quantitites as a function of the various parameters defining the structure of the cross section.

The configuration which is discussed in this correspondence is shown in Fig. 1: two parallel ground planes with a spacing g between them. Centered between these ground

Manuscript received January 31, 1967; revised April 11, 1967.

[1] H. E. Green, "The numerical solution of some important transmission line problems," *IEEE Trans. Microwave Theory and Techniques*, vol. MTT-13, pp. 676–692, September 1965.
[2] M. V. Schneider, "Computation of impedance and attenuation of TEM lines by finite difference methods," *IEEE Trans. Microwave Theory and Techniques*, vol. MTT-13, pp. 793–800, November 1965.